

MECHANICAL PROPERTY-MICROSTRUCTURAL RELATIONSHIPS IN ABALONE SHELL*

M. SARIKAYA, K. E. GUNNISON, M. YASREBI, and I. A. AKSAY

Department of Materials Science and Engineering, and
Advanced Materials Technology Program, The Washington Technology Center,
University of Washington, Seattle, WA 98195

The microstructure and mechanical properties of abalone shell were studied. It was found that fracture strength, σ_f , is 180 MPa, and fracture toughness, K_{IC} , is $7 \pm 3 \text{ MPa}\cdot\text{m}^{1/2}$; these values are comparable with or better than most "high technology" ceramic materials. The microarchitecture of the nacre section of the red abalone shell is similar to a "brick and mortar" structure, where CaCO_3 is the brick and organic matter is the mortar, constituting 95% and 5% of the microstructure by volume, respectively. This impressive combination of σ_f and K_{IC} values is attributed to the laminated structure of the shell with hard and thick ($0.25 \pm 0.5 \mu\text{m}$) CaCO_3 and superplastic and thin (20-30 nm) organic components. Although there are several toughening mechanisms operating in the shell, fractographic studies identified sliding of CaCO_3 layers and bridging by the organic layers to be the most effective ones. These phases also have a strong interface. The results of our experiments are discussed in the context of using abalone shell as a model for the design of synthetic laminates such as cermet (ceramic-metal) and cerpoly (ceramic-polymer) composites.

INTRODUCTION

In the quest to develop tailor-made materials that possess certain physical properties, novel processing techniques are developed to control the complete microstructural evolution down to the nanometer scale. Some recent studies indicate that materials with controlled microstructural variations at this ultrastructural level exhibit unprecedented mechanical, electrical, superconductive, and optical properties [2-5]. The most notable of these properties are (i) the supermodulus effect (i.e., increase in modulus of elasticity) [2] in laminated materials where the laminate thickness is in the 1.5-5 nm range; and (ii) high temperature superconducting materials (e.g., $\text{YBa}_2\text{Cu}_3\text{O}_{7-x}$) [6], where the correlation length is 1.0-1.5 nm. The processing of these synthetic materials is based on the additive principle, in which the component phases with different properties are fused together in an ordered manner to form a multiphase system. Traditionally, the microstructures of these synthetic materials can be achieved by (i) phase transformations, such as those seen in eutectic and eutectoid systems (e.g., $\text{Al-Cu}_2\text{Al}$ and $\text{Fe-Fe}_3\text{C}$, respectively) [7]; (ii) mechanical mixing of component phases (e.g., metal and ceramic matrix composites); and (iii) tape casting and infiltration (e.g., in cermet and cerpoly systems). However, in these cases, microstructural control is difficult. Other, more advanced processing involves ion beam techniques (such as molecular beam epitaxy) and liquid and vapor infiltration/deposition. With these techniques, the microstructure is controlled at the nanometer level, but the size of the materials that could be produced is extremely limited, and therefore, they do not have widespread application, except for electronic materials. In order to meet the demands of modern technology for materials with better properties, larger materials with complex shapes have to be developed through more intricate and energy-efficient strategies.

The approach used by living organisms in processing composites is in many ways more controlled than the synthetic methods. In the formation of biological composites, living or-

* Summary of a paper to be submitted to *J. Mater. Res.* (1990).

ganisms can efficiently design and produce more complex microstructures with unique properties at many spatial levels (down to the nanometer scale) and with greater control [8-11]. Such examples include magnetite (Fe_3O_4), produced by the freshwater magnetotactic bacteria, *Aquaspirillum magnetotacticum* [12]. Magnetite has an average size of 500 Å, well in the single domain region [13], with a perfect lattice structure, thereby enhancing its magnetic property (discussed elsewhere in these proceedings). Other examples include the complex structures of organic/inorganic composite mixtures, such as exoskeletons of invertebrates and the skeleton and teeth of vertebrates, which possess excellent mechanical properties [8,11].

It is desirable, therefore, to produce manmade materials by using the processing approaches and design principles similar to those used by living organisms, i.e., biomimicking. The present research has been initiated to study the principles inherent in the processing methods used by living organisms in producing composites and the physical properties of the composites as related to their microstructures.

The objectives of this paper are (i) to summarize some of the findings regarding microstructure-property relationships in an abalone shell, (ii) discuss possible toughening mechanisms for these composites on the basis of fractographic studies, and (iii) derive guidelines from this study for the design of synthetically laminated materials.

EXPERIMENTAL

The *Haliotis rufescens* (red abalone) was collected in the Pacific Ocean west of Baja California, and all studies discussed here were performed on adult (~10 years of age) specimens. The shells were 25-30 cm in diameter, with a thickness in the nacre layer of 0.5-1.0 cm. The mechanical tests were performed within 5 weeks following the removal of the abalone from the ocean.

Mechanical tests were conducted by using bar specimens with square cross-sections. Fracture strength, σ_f , and fracture toughness, K_{IC} , tests were performed on single straight notched samples in 4-point and 3-point bending modes, respectively. Similar tests were also done on polycrystalline $\alpha\text{-Al}_2\text{O}_3$ samples and plotted in Fig. 1 as a comparison.

Fractographic studies were done either on the fractured samples or on microhardness indented samples (to study crack propagation) using a scanning electron microscope (SEM). Ultramicrostructural analysis of the shell was performed by transmission electron microscopy (TEM) (Philips 430T) on ion-milled samples (details of the sample preparation are discussed in Ref. 1).

RESULTS

(a) Microstructure

A longitudinal cross-section of the red abalone shell (*Haliotis rufescens*) displays two types of microstructures: an outer prismatic layer and inner nacreous layer. Two forms of CaCO_3 , calcite (rhombohedral, $R\bar{3}c$) and aragonite (orthorhombic, Pmnc), constitute the inorganic component of the composite in the prismatic and nacreous layers, respectively. The structure and properties of the nacreous layer are described here, since it is this part of the shell that displays a good combination of mechanical properties as a result of its unique laminated microstructure.

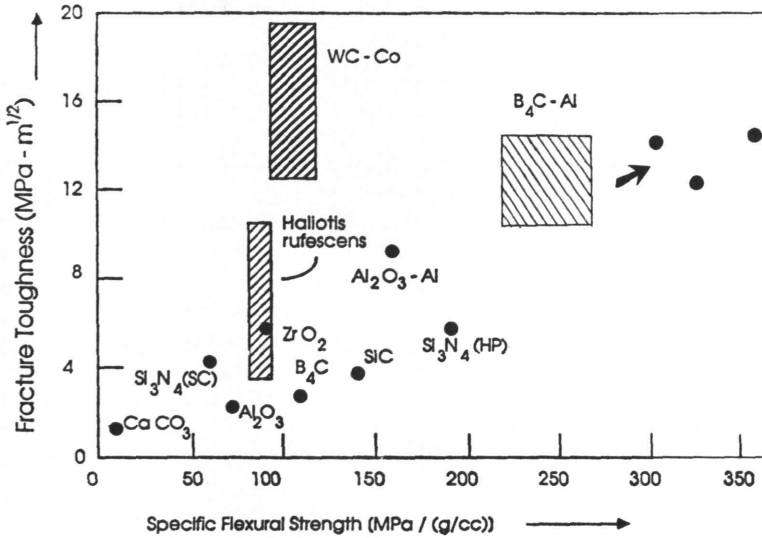


Fig. 1. Fracture toughness versus fracture strength (specific) of the nacre section of the abalone shell compared to some high technology ceramic and cermet materials.

Figure 2, a TEM bright-field image, shows the microstructure of the nacreous layer in which the CaCO₃ layer is about 0.25-0.5 μm and the organic layer is 20-50 nm. The CaCO₃ “bricks” are single crystals, and there are specific orientation relationships among the crystals in the same layer, as well as among crystals in successive layers. The organic layer, the molecular composition of which is not well understood, is continuous between the CaCO₃ layers.

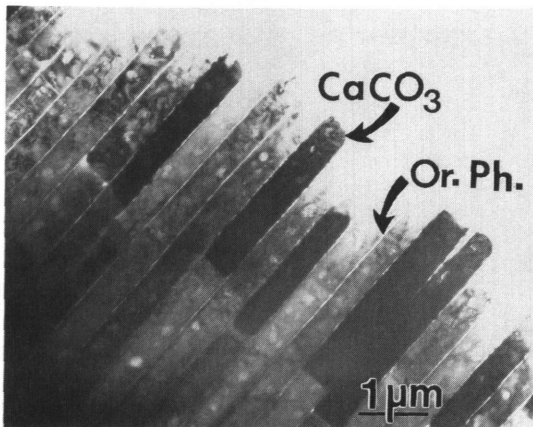


Fig. 2. Bright field image (TEM) of the cross-section of nacre (end-on orientation) showing aragonite “bricks” and organic phase “mortar”.

(b) Mechanical Properties and Fractography

Both the fracture strength, σ_f , and fracture toughness, K_{IC} , values have been evaluated in the transverse direction, i.e., perpendicular to the shell plane. The average σ_f value is 185 ± 20 MPa and K_{IC} is 8 ± 3 MPa-m^{1/2}. As indicated, both the strength and the toughness values show a scatter, especially in the latter case. This is due to natural defects in the nacre and the somewhat curved shape of the layers. Nonetheless, the combination of these properties qualifies abalone shell as a high performance material, as shown in the toughness-strength diagram (Fig. 1).

The observation of the crack propagation behavior reveals a high degree of tortuosity not seen in the more traditional brittle ceramics (such as Al₂O₃) or the high toughness ceramics (such as ZrO₂) [14]. A microstructure showing the tortuous crack propagation of the abalone shell is displayed in Fig. 3. The most apparent feature of the crack propagation seen in the SEM micrographs is crack blunting/branching and microcrack formation. A closer examination of the fractographs reveals, however, that the microcracks advance both on planes parallel to the CaCO₃ layers and across those layers. However, it is not clear whether the cracks propagate inside the organic layer or through the interface plane between the organic and inorganic components.

The surface of the fractured sample (seen in Fig. 4) indicates that the major crack has meandered around the CaCO₃ layers, passing through the organic layers, and has resulted in a highly rough surface with partially exposed plates.

In micrographs taken at much higher magnification, separation of the CaCO₃ layers in both \vec{x} and \vec{y} directions (in the layer plane) is clearly seen (Fig. 5). The “bricks” have been left intact, which may indicate that they “slide” on the organic layer. The higher magnification micrograph in Fig. 6, on the other hand, displays organic ligaments which are stretched (in the perpendicular direction, i.e., the \vec{z} direction) between the CaCO₃ layers. This stretching indicates that the interface between the organic and inorganic phases is strong and that the organic phase acts as a strong binder.

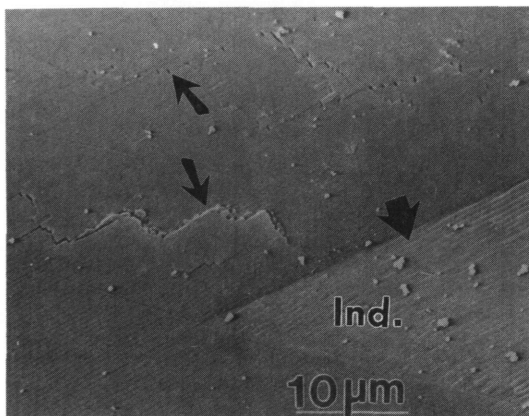


Fig. 3. Scanning electron image (SEM) of the polished surface of the shell showing the crack propagation behavior around a micro-indentation (Ind.) High tortuosity and microcrack formations are clearly revealed.

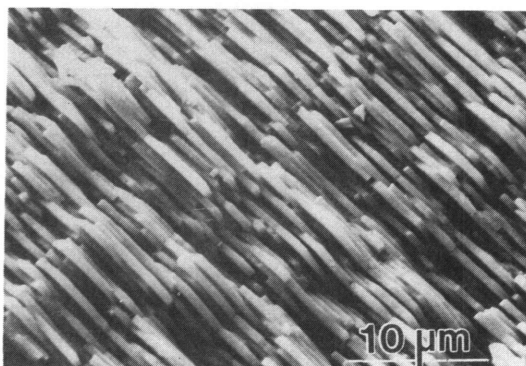


Fig. 4. SEM micrograph (SE) of the fractured surface of a test sample showing "plate pull-out" and resulting high tortuosity.

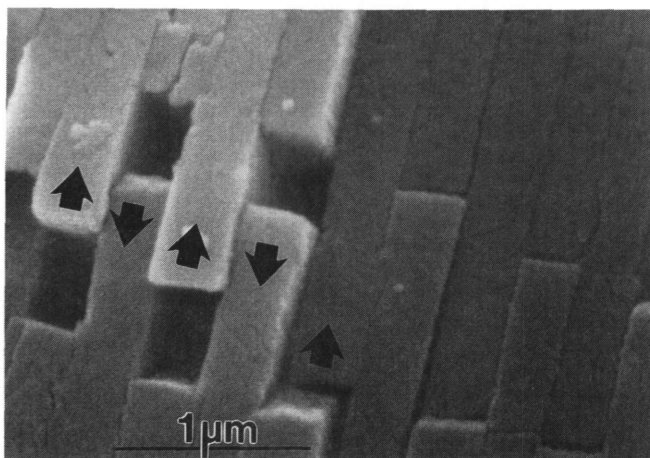


Fig. 5. SEM micrograph (SEM) clearly reveals sliding in the direction of the arrows (i.e., in the plane of the layers).

Preliminary results [15] on the mechanical properties of B_4C -Al (35 vol%) laminated cermets designed and processed on the basis of the above observations indicate a 30% increase in the fracture toughness of the composite (Fig. 1). An SEM image of the fracture surface of the B_4C -Al laminate is shown in Fig. 7. The increase in the cermet toughness is attributed to the same toughening mechanisms observed in abalone shell. Further improvement in both strength and toughness is expected with a decrease in the thickness to submicrometer levels of the composite layers; in the present case, the minimum thickness of the layers in the cermet laminate is about $10\ \mu\text{m}$, far too thick to benefit from the effects of the type of lamination seen in abalone shell. Consequently, our present research is directed to the processing of cermets with submicrometer-layer thicknesses in conjunction with studies of the quantitative effects of the organic layer in sea shells.

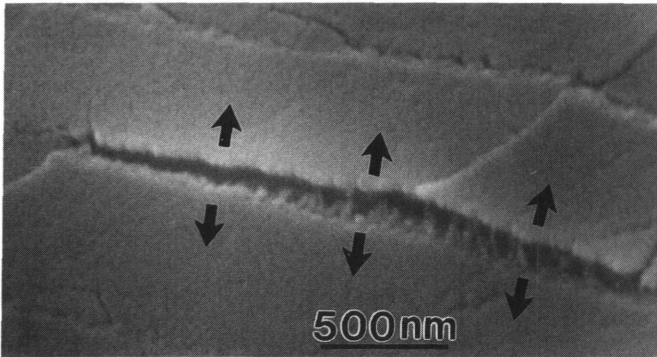


Fig. 6. SEM micrograph (SE) showing the organic ligament formation between the CaCO₃ layers when resolved stresses are in the direction shown by the arrows.

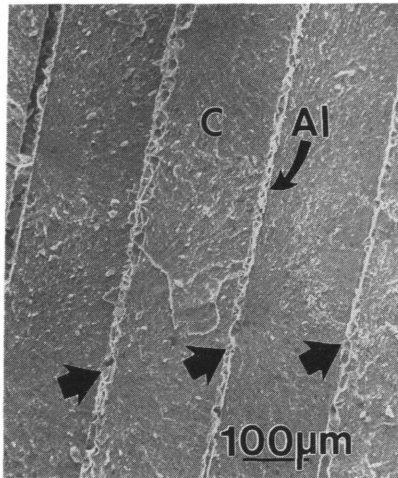


Fig. 7. SEM image of the fractured surface of the B₄C-Al/Al composite. B₄C-Al is indicated by C. Broad arrows show strong interfaces, open arrow shows weak interface.

DISCUSSION AND SUMMARY

The fracture behavior of the abalone shell and that of commonly used monolithic ceramic materials have been compared in terms of crack propagation. An indentation experiment (for example, the Vickers hardness test) performed in polycrystals of alumina and partially stabilized zirconia show that these ceramics exhibit straight cracks extending radially from the corners of the indentation, indicating brittle behavior. Indentation in the transverse direction in the nacreous layers in abalone shell indicates that cracks do not extend from the corners of the

indentation, but from regions close to the corners in various directions (Fig. 3). These directions are probably the high strain regions formed by the complex stress distribution in the shell structure. The formation of tortuous cracks and microcracks (Figs. 3-5) is an indication of a high degree of energy absorption in the form of deformation during crack propagation, resulting in a higher fracture toughness compared to monolithic ceramics.

Fractographic analysis of the fracture surfaces and indentation cracks reveals several possible toughening mechanisms. These are (i) crack blunting/branching, (ii) microcrack formation, (iii) pull-outs (plates), (iv) crack bridging (ligament formation), and (v) sliding of layers. It would be desirable for all of these mechanisms to be operative in a composite in order to increase fracture toughness and strength. The high tortuosity seen here in crack propagation is due mainly to crack blunting and branching. However, tortuosity is not the major toughening mechanism in these composites. The linear tortuosity, determined from a number of indentation cracks, indicates a 30-50% value. Although linear tortuosity may contribute, it cannot be the major mechanism for the more than 20-fold increase in toughness.

There are similarities between the deformation of a nacreous sea shell and a metal. These may be stated as follows:

(i) Around the periphery of the indentation (as seen in Fig. 3), the material exhibits deformation features, such as sliding of CaCO_3 layers to accommodate the strain caused by the indenter. These deformation features are similar to the Lüders bands (or slip bands) seen in metals (such as in face-centered cubic Cu and Ni) caused by the dislocation slip which accommodates the applied stress on high atomic density planes (such as {111}). It is also noted that the degree of sliding near the indentation is higher and it decreases with distance from the indentation.

(ii) As the sliding takes place to accommodate deformation, there is no cracking through the layers except for microcrack formation. This indicates that the biocomposite is not brittle and the strain accommodation mostly takes place between CaCO_3 layers, not through the ceramic layers. At this stage, however, it is not known whether the biopolymer layer at the interface between the ceramic and biopolymer is ruptured. Nonetheless, this complex deformation mode increases the toughness of the composite.

Sliding takes place, probably, when there is a resolved shear stress acting in the plane of the layers. However, if the resolved stress has a tensile component (normal to the layers) then the CaCO_3 layers are forced to separate. This separation is resisted by the formation of organic ligaments which are stretched across the organic layers and form bridges between the CaCO_3 plates. It should be noted here that the organic matrix has a plywood-like structure [11]. The fact that there is a 1000% deformation of the organic layer and that the organic layer is still intact is due to the strong interface between the organic and inorganic phases in the shell and the ultrastructure of the organic layer.

In order to aid the design of future synthetic laminated materials, three guidelines may be drawn from the present analysis: (i) lamination of the component phases should form a highly ordered microarchitecture; (ii) mechanical properties of the component phases should be such that the thick phase should be hard, and the thin phase should be soft; (iii) interfaces should be strong. Therefore, the property requirements for soft phase imply that it be highly plastic, while the thick phase should have a high hardness.

In the design of synthetic laminates, high hardness ceramics, such as BN, B_4C , TiC, etc., can be taken as the hard component. Highly plastic (superplastic) metals and alloys, such as

Al or Cu (and their alloys) may be good candidates for the soft component, provided that they can be processed and would result in strong interfaces. These requirements are met to a certain degree in the B_4C -Al laminate system (Fig. 7), but further modifications are necessary in processing to obtain finer layers with stronger interfaces.

ACKNOWLEDGMENTS

This research was supported by the Air Force Office of Scientific Research under Grant Nos. AFOSR-87-0114 and AFOSR-89-0496. The assistance of D. L. Milius in the mechanical property measurements is gratefully acknowledged.

REFERENCES

1. M. Sarikaya, K. E. Gunnison, and I. A. Aksay, "Sea-Shells as a Natural Model to Study Laminated Materials," to be submitted to *J. Mater. Res.* (1990).
2. F. Spaen, "The Art and Science of Microstructural Control," *Science*, **235**, 1010 (1987).
3. R. C. Cammarata, "The Supermodulus Effect in Composition Modulated Thin Films," *Scripta Met.*, **20**, 883 (1980).
4. M. S. Dresselhaus, "Intercalation of Layered Materials," *Mater. Res. Bull.*, **12** [3] 24 (1987).
5. *Metallic Superlattices: Artificially Strong Materials*, edited by T. Sinjo and T. Takada (Elsevier, Amsterdam, 1987).
6. See, for instance, J. D. Jorgensen et al., "Structural and Superconducting Properties of Orthorhombic and Tetragonal $YBa_2Cu_3O_{7-x}$: The Effect of Oxygen Stoichiometry and Ordering on Superconductivity," *Phys. Rev. B*, **36**, 5731 (1987).
7. A. Kelly and R. L. Nicholson, *Strengthening Methods in Crystals* (Wiley, New York, 1971).
8. a. H. A. Lowenstam, "Minerals Formed by Organisms," *Science*, **211**, 1126 (1981); b. H. A. Lowenstam and S. Weiner, *On Biomineralization* (Oxford University Press, Oxford, 1989).
9. a. S. Mann, "Mineralization in Biological Systems," *Structure and Bonding*, **54**, 124 (1983); b. *Biomineralization: Chemical and Biochemical Perspectives*, edited by S. Mann, J. Webb, and R. J. Williams (VCH Publishers, Weinheim, 1989).
10. S. Weiner, "Organization of Extracellularly Mineralized Tissues: A Comparative Study of Biological Crystal Growth," *CRC Critical Reviews in Biochemistry*, **20** [4] 365 (1986).
11. a. *The Mechanical Properties of Biological Materials*, edited by J. A. Currey and J. F. V. Vincent (Cambridge Univ. Press, Cambridge, 1980); b. J. D. Currey, "Biological Composites", *J. Materials Educ.*, **9** [1-2] 118 (1987).
12. R. P. D. Blakemore and R. S. Wolfe, "Isolation and Fine Culture of a Freshwater Magnetic *Spirillum* in Chemically Defined Medium," *J. Bacteriol.*, **140**, 720 (1979).
13. I. S. Jacobs and C. P. Bean, "An Approach to Elongated Fine Particle Magnets," *Phys. Rev.*, **100**, 1060 (1955).
14. *Deformation of Ceramic Materials II*, edited by R. C. Tressler and R. C. Bradt (Plenum, New York, 1984).
15. M. Yasrebi and I. A. Aksay, "Processing of Laminated B_4C -Al Cermets," unpublished results, University of Washington, Seattle (1989).